Fish CDK2 recruits Dtx4 to degrade TBK1 through ubiquitination in the antiviral response

Long-Feng Lu[a,c], Can Zhang[a,c], Zhuo-Cong Li[a,c], Bao-Jie Cui[a,f], Yang-Yang Wang[a,c], Ke-Jia Han[a,f], Xiao Xu[a,f], Chu-Jing Zhou[a,f], Xiao-Yu Zhou[a,c], Yue Wu[a,c], Na Xu[a,c], Xiao-Li Yang[a,c], Dan-Dan Chen[a,c], Xi-Yin Li[a,c,d,e], Li Zhou[a,c,d,e], Shun Li[a,b,c,d,e 1]

[a]Institute of Hydrobiology, Chinese Academy of Sciences, Wuhan, China

[b]Laboratory for Marine Biology and Biotechnology, Qingdao Marine Science and Technology Center

[c]University of Chinese Academy of Sciences, Beijing, China

[d]State Key Laboratory of Freshwater Ecology and Biotechnology, Institute of Hydrobiology

[e]Key Laboratory of Aquaculture Disease Control, Ministry of Agriculture, Wuhan, China

[f]College of Fisheries and Life Science, Dalian Ocean University, Dalian, China

[1] Corresponding author. Email: bob@ihb.ac.cn

Abstract

Although the classical biological protein cell cycle protein kinase CDK2 has been extensively studied in higher vertebrates, its function in lower vertebrates beyond the regulation of mitosis remains unknown. In this study, we report a distinct mechanism whereby IFN expression is negatively regulated in fish by CDK2. After infection with the spring viremia of carp virus (SVCV), fish CDK2 expression significantly increased in tissues and cells. Moreover, antiviral resistance was improved in *cdk2*$^{-/-}$ homozygotes, and the antiviral cytokine interferon (IFN) expression was significantly higher. At the cellular level, CDK2 overexpression reduced IFN expression, while *cdk2* knockdown increased the ability of cells to produce IFN. Subsequently, it was discovered that fish CDK2 binds and degrades TBK1, resulting in reduced IFN. CDK2 increases the K48-linked ubiquitination of TBK1, causing its degradation, while E3 ubiquitin ligase Dtx4 was found to be involved in this process following the significant enhancement of TBK1 K48-linked ubiquitination. Protein mass spectrometry and immunoblot analysis confirmed that the K567 site on TBK1 is essential for CDK2 to engage with Dtx4 and degrade TBK1; thus, after mutating the K567 site, K48-linked ubiquitination of TBK1 was not enhanced by Dtx4, and TBK1 was not degraded by CDK2. Our data demonstrate that fish CDK2 recruits the E3 ubiquitin ligase Dtx4 to target the K567 site of TBK1 and promote its degradation. These results suggest that CDK2 in lower vertebrates is implicated in a specialized role for antiviral innate immunity.

Introduction

Interferon (IFN) production is central to the host's innate immune response to viral infections. IFN acts as a ligand, binding to receptors on neighboring cell membranes through the autocrine and paracrine pathways, which initiates the Janus kinase/signal transducer and activator of the transcription (JAK/STAT) signaling pathway [1]. This, in turn, leads to the transcription of a large number of antiviral genes, ultimately resulting in the clearance of intracellular viral components [2]. IFN induction depends on cellular pattern recognition receptors (PRRs) and sensing of conserved pathogen-associated molecular patterns (PAMPs), with the retinoic acid-inducible gene I (RIG-I)-like receptors (RLRs) signaling pathway being critical in this system [3]. Viral nucleic acids are recognized by the RLRs, which then initiate a series of signaling events that lead to downstream IFN expression. TANK-binding kinase 1 (TBK1) efficiently phosphorylates IFN regulatory factor 3/7 (IRF3/7), facilitating its nuclear entry [4].

Effective control of IFN production is crucial during viral infection in maintaining immune responses and homeostasis, whereby excessive IFN can cause inflammatory storms that harm the organism. Hence, TBK1 plays a significant role in the IFN signaling pathway and is negatively regulated by various factors to balance IFN expression in the host [5]. Mammalian TBK1 is degraded by NLRP4, which recruits the E3 ubiquitin ligase DTX4 for K48-linked polyubiquitination at Lys670 [6]. Additionally, DYRK2 is crucial in the degradation of TBK1 by NLRP4 through the phosphorylation of Ser527, as mentioned in previous studies [7, 8]. The function of TBK1 is conserved in fish and subject to modulation by multiple molecules to prevent excessive IFN expression. Indeed, TMEM33 in zebrafish serves as a TBK1 substrate, reducing IRF3 phosphorylation and hindering TBK1 kinase activity to diminish IFN expression [9]. Generally, the ability of TBK1 to induce IFN is conserved and tightly regulated within the host.

CDKs are a family of Ser/Thr kinases that act as cell cycle regulators. Cell cycle progression from the G1 phase to the S phase and from G2 to mitosis is controlled by various cyclin–CDK complexes. For example, CDK2 and cyclin E regulate the G1–S

transition [10]. Further studies have unveiled other functions of the CDK family in biological processes beyond cell cycle regulation. The transcription of multiple proinflammatory genes is upregulated in a CDK-dependent fashion throughout the G1 phase [11]. In the context of antitumor immunity in fibrosarcoma and lung carcinoma, inhibiting CDK2 leads to the RB protein being phosphorylated, which results in increased production of type I IFN [12]. Another study demonstrated that inhibiting CDKs or the knockdown of CDKs activities caused a significant blockade in IFN release from culture supernatants [13]. While there are several reported functions of CDKs in innate immunity, understanding the roles of CDKs in this area remains unclear.

The immune systems of higher vertebrates (e.g., humans) and lower vertebrates (e.g., fish) generally exhibit some consistency, although there are notable differences. For instance, IFN phosphorylates fish IRF3, which is only phosphorylated by viruses in mammals. Additionally, fish MVP functions as an IFN-negative regulator, while human MVP mediates IFN-positive expression [14, 15, 16, 17]. There are 13 CDK genes in the human genome and 21 CDK orthologs in zebrafish, indicating that CDK functions are conserved and differ between fish and humans. Our report reveals that fish CDK2 acts as an IFN negative regulator that recruits Dtx4 to facilitate the ubiquitination of TBK1, thereby restricting IFN expression. These findings offer valuable insights into the various roles of CDK2.

Results

1. CDK2 is upregulated during viral infection *in vivo* and *in vitro*

To identify potential molecules linked with viral infection, we generated a transcriptome pool from liver and spleen tissues taken from SVCV-infected zebrafish. Notably, classical cell cycle regulator *cdk2* was among the few upregulated genes in the CDK family (Fig. 1 *A* and *B*). In previous studies, it was found that mammalian *cdk2* was not regulated during viral infection. As shown in Figure 1C, this was confirmed by detecting *cdk2* after THP-1 cells infection with VSV, and it was observed that *cdk2* was not upregulated. Fish *cdk2* was significantly increased upon infection with fish viruses

118 CyHV-2 or SVCV in *Carassius auratus gibelio*, *Danio rerio*, and *Pimephales promelas*,
119 compared to human *cdk2*, indicating that fish CDK2 is involved in the host's antiviral
120 response. Meanwhile, specific qPCR and immunoblot analysis to validate this finding
121 in zebrafish tissues, which demonstrated that the *cdk2* transcript level was significantly
122 increased upon SVCV infection. The CDK2 protein level was also consistently higher
123 in the viral infection group (Fig. 1 *D* and 1 *E*). We investigated whether this CDK2
124 expression pattern also existed *in vitro*. For this purpose, we used the zebrafish
125 embryonic fibroblast cell line (ZF4) and another cyprinid fish cell line (epithelioma
126 papulosum cyprini (EPC)). During the 48-hour (h) viral infection period, CDK2 was
127 significantly upregulated at the protein level (Fig. 1 *F*). Taken together, the *in vivo* and
128 *in vitro* data suggest that fish CDK2 may play a role in the response to viral infection.
129

130 **2. *cdk2*$^{-/-}$ fish exhibit effective antiviral capacities**

131 To investigate the role of CDK2 in the antiviral process, we generated a *cdk2*
132 knockout zebrafish homozygote (*cdk2*$^{-/-}$). Our findings demonstrated that the survival
133 rate under viral infection was significantly higher in the *cdk2*$^{-/-}$ group than in the wild-
134 type group (Fig. 2 *A*). We selected the liver, spleen, and kidney as representative tissues
135 in which to analyze the *cdk2*$^{-/-}$ antiviral capacity. In the H&E staining assay, severe
136 tissue damage was observed in the wild-type group, while the *cdk2*$^{-/-}$ group displayed
137 dramatically less tissue damage (Fig. 2 *B*). The viral transcripts in these tissues were
138 observed and then compared to the abundance in the wild-type. The replication of viral
139 genes, such as SVCV N, was typically inhibited in *cdk2*$^{-/-}$ homozygote tissues (Fig. 2
140 *C*). Viral protein level analysis also confirmed these results, as SVCV G, N, and P
141 proteins were suppressed in *cdk2*$^{-/-}$ homozygotes (Fig. 2 *D*).

142 Transcriptomics analysis was employed to investigate the antiviral regulation by
143 CDK2. Differential expression analysis identified 1707 upregulated genes and 1490
144 downregulated genes in the liver of *cdk2* knockout zebrafish versus WT zebrafish after
145 SVCV infection (Fig. 2 *E*). Moreover, gene set enrichment analyses (GSEAs) were
146 performed to analyze the IFN response to virus infection-related genes, which
147 demonstrated that these genes were significantly activated in the *cdk2*$^{-/-}$ group (Fig. 2

148 *F*). Differential expression analysis further showed that *cdk2* knockout results in the
149 upregulation of many IFN-stimulated genes (ISGs) after SVCV infection (Fig. 2 *G*). To
150 procure the transcriptome data, IFN was assayed in zebrafish tissues, including liver,
151 spleen, and kidney. Similar to in the transcriptome assay, IFN was found to be
152 significantly higher in the *cdk2*$^{-/-}$ groups, indicating that stronger antiviral capacity and
153 higher IFN transcription occurred in *cdk2*$^{-/-}$ fish (Fig. 2 *H*). Collectively, these data
154 suggest that viral replication was hindered in the *cdk2*$^{-/-}$ fish.
155
156 **3. CDK2 inhibits IFN expression and promotes viral proliferation**
157 The impact of CDK2 on viral infection was examined in relation to IFN. The IFN
158 response is an essential mechanism for host resistance against viruses. Overexpression
159 of CDK2 decreased the IFN promoter and ISRE motif activation by SVCV or poly I:C
160 (Fig. 3 *A*). An effective shcdk2 was produced and identified (Fig. 3 *B*). The impact of
161 CDK2 knockdown was explored, with the results suggesting that the downregulation
162 of CDK2 facilitates IFN promoter activity (Fig. 3 *C*). The mRNA levels of *ifn* and
163 downstream ISG *vig1* transcription were monitored, revealing that CDK2 caused a
164 significant decrease in *ifn* and *vig1*, whereas the knockdown of CDK2 increased the
165 IFN response (Fig. 3 *D*). In the antiviral capacity assays, CDK2 from zebrafish, gibel
166 carp, and grass carp all promoted the proliferation of their respective corresponding
167 viruses (Fig. 3 *E*). Conversely, CDK2 knockdown significantly suppressed viral
168 proliferation (Fig. 3 *F*). Cells overexpressing CDK2 showed enhanced production of
169 viral mRNA and proteins, while CDK2-knockdown cells showed attenuation of the
170 same viral mRNA and proteins (Fig. 3 *G* and *H*). Immunofluorescence revealed a higher
171 intensity of green signals indicating SVCV N protein in the CDK2 overexpression
172 group compared to the control, while a lower green signal was observed in the CDK2-
173 knockdown group compared to the normal group (Fig. 3 *I*). These findings suggest that
174 CDK2 inhibits IFN expression in the host and reduces antiviral capacity.
175
176 **4. CDK2 interacts with TBK1 and reduces its expression**
177 The RLR pathway plays an important role in IFN activation. To investigate

178 whether CDK2 counters RLR signaling, as observed earlier, we examined whether
179 CDK2 inhibits RLR factors that activate IFN promoters. The activation of the IFN
180 promoters induced by MAVS and TBK1 was significantly inhibited by CDK2, whereas
181 it was unaffected by MITA (Fig. 4 *A*). CDK2 knockdown restored MAVS and TBK1
182 functions following IFN promoter stimulation (Fig. 4 *B*). Moreover, the *ifn* and *vig1*
183 transcripts were monitored. The results showed that CDK2 notably reduced *ifn* and *vig1*
184 mRNA levels, whereas the CDK2 knockdown improved the IFN response (Fig. 4 *C* and
185 *D*). These findings suggest that CDK2 targets either MAVS or TBK1. The subcellular
186 localization of CDK2 was observed to be distributed throughout the cell. However,
187 TBK1 and MAVS exhibited cytoplasmic localization, while there appeared to be a
188 significant punctate overlap between CDK2 and TBK1, indicating a possible
189 association between CDK2 and TBK1 (Fig. 4 *E*). Subsequently, association analysis of
190 CDK2 and MAVS or TBK1 was conducted. The co-IP assay revealed an interaction
191 between CDK2 and TBK1, yet not between CDK2 and MAVS (Fig. 4 *F*). Afterward,
192 an endogenous co-IP assay was performed to confirm the interaction between CDK2
193 and TBK1, while the interaction was also verified with TBK1 or CDK2 being enriched
194 (Fig. 4 *G*). To identify the essential domain that mediates the interaction with CDK2,
195 two truncated TBK1 mutants were generated (Fig. 4 *H*). The TBK1-ΔN-flag, which
196 lacked the kinase domain, meaning it cannot bind to CDK2, indicated that the kinase
197 domain in TBK1 is necessary for it to associate with CDK2 (Fig. 4 *I*). Since the
198 interaction between CDK2 and TBK1 was confirmed, whether CDK2 affects TBK1
199 stability was also investigated. Co-overexpression of the relevant RLR factors and
200 CDK2 demonstrated that TBK1 expression was substantially decreased in the presence
201 of CDK2, compared to MAVS (Fig. 4 *J*). Consistently, CDK2 impaired endogenous
202 TBK1 under both normal and stimulation states, whereas CDK2 knockdown abolished
203 this effect, indicating that CDK2 impaired TBK1 expression (Fig. 4 *K* and *L*). The
204 expression of TBK1 was also significantly increased in the liver, spleen, and kidney of
205 *cdk2*$^{-/-}$ fish, confirming the *in vivo* impact of CDK2 on TBK1 expression (Fig. 4 *M*).
206 Subsequently, its biological function was studied to investigate whether CDK2 affects
207 the crucial antiviral role of TBK1. During SVCV infection, cells overexpressing TBK1

208 showed little CPE; however, CDK2 dramatically counteracted the antiviral capacity of
209 TBK1, as confirmed by virus titer identification (Fig. 4 *N*). For viral protein expression,
210 CDK2 restored the TBK1-mediated prevention of viral protein expression, including
211 SVCV G, N, and P proteins. Immunofluorescence also demonstrated that the inhibition
212 of SVCV N protein by TBK1 was restored following CDK2 overexpression (Fig. 4 *O*
213 and *P*). CDK2 also restored viral nucleic acid transcription, which was abolished by
214 TBK1 (Fig. 4 *Q*). These results demonstrate that CDK2 interacts with the kinase domain
215 in TBK1, leading to reduced expression and a weakened antiviral effect.
216

217 **5. CDK2 causes TBK1 degradation by increasing K48-linked polyubiquitination**

218 The next step was to investigate the mechanisms through which CDK2 negatively
219 regulates TBK1. To determine whether the decrease in TBK1 occurred at the mRNA or
220 protein level, *tbk1* transcription was monitored. CDK2 had little effect on *tbk1* in either
221 the control or virus-infected groups (Fig. 5 *A*). Therefore, attention was placed on
222 modulating TBK1 at the protein level. Various reagents that inhibit the ubiquitin (Ub)-
223 proteasome and autophagosome, such as MG132, 3-MA, Baf-A1, and CQ, were
224 utilized to clarify the precise regulatory mechanism. Compared to the autophagosome
225 inhibitors 3-MA, Baf-A1, and CQ, using the Ub-proteasome inhibitor MG132
226 significantly impeded TBK1 degradation in a dose-dependent manner (Fig. 5 *B* and *C*).
227 This suggests that the degradation of TBK1 by CDK2 is proteasome-dependent. Similar
228 results were observed for endogenous TBK1 in the presence or absence of poly I:C
229 stimulation or SVCV infection (Fig. 5 *D*). Since ubiquitination is an important process
230 during proteasome-dependent degradation, we next investigated whether ubiquitination
231 was important in the CDK2-mediated degradation of TBK1. Expectedly, immunoblot
232 analysis confirmed that CDK2 increased the ubiquitination of TBK1 (Fig. 5 *E*).
233 Polyubiquitin chain modification, either K48-linked or K63-linked, can either target
234 proteins for degradation or increase stability. To investigate how TBK1 was modified,
235 we performed MS analysis of ubiquitinated TBK1 from cells and found that K48-linked
236 polyubiquitinated TBK1 was readily detected in CDK2-overexpressed cells, whereas
237 K63-linked polyubiquitinated TBK1 was hardly detected (Fig. 5 *F*). Consistently, when

238 we transfected EPC cells with TBK1-Myc, CDK2-HA, WT-Ub, K48-Ub, or K63-Ub,
239 we found that CDK2 markedly increased K48-linked, but not K63-linked,
240 ubiquitination of TBK1, while CDK2 knockdown remarkably attenuated K48-linked
241 ubiquitination of TBK1 (Fig. 5 *G* and *H*). Taken together, these findings indicate that
242 the CDK2 triggers the degradation of TBK1 through K48-linked ubiquitination.
243
244 **6. CDK2 recruits the ubiquitin E3 ligase Dtx4 to interact with and degrade TBK1**
245 Since CDK2 is not an E3 ubiquitin ligase, it is speculated that CDK2-mediated
246 degradation of TBK1 does not occur directly; instead, CDK2 acts as an adaptor to
247 recruit an E3 ubiquitin ligase to TBK1. Several homologs of TBK1-associated E3
248 ubiquitin ligases in mammals were cloned into fish to detect protein interactions. It was
249 found that Trim11 and Dtx4 are associated with TBK1, and these interactions were
250 verified through inverse experiments (Fig. 6 *A and B*). Moreover, protein interactions
251 between CDK2 and Trim11 or Dtx4 were investigated. Dtx4 exhibited a significant
252 interaction with CDK2 but not with Trim11, indicating that Dtx4 interacts with both
253 TBK1 and CDK2 (Fig. 6 *C*). Hence, Dtx4 was the main focus of the subsequent assays.
254 Since Dtx4 is a potential ubiquitin ligase for TBK1, we verified whether CDK2
255 facilitated the interaction between Dtx4 and TBK1. Overexpression of CDK2
256 significantly increased the interaction between Dtx4 and TBK1, while CDK2
257 knockdown impeded this progress, suggesting that CDK2 promotes the interaction
258 between Dtx4 and TBK1 (Fig. 6 *D*). Next, the impact of the Dtx4 interaction was
259 elucidated. Overexpression of DTX4 amplified CDK2-mediated inhibition of IFN
260 promoter activity induced by TBK1 (Fig. 6 *E*). Moreover, CDK2-mediated reduction
261 of *ifn* and *vig1* mRNAs activated by TBK1 was also augmented by Dtx4 overexpression
262 (Fig. 6 *F*). In contrast to the normal state where CDK2 degrades TBK1, Dtx4
263 overexpression increased degradation (Fig. 6 *G*). The degradation of endogenous TBK1
264 by CDK2 was more severe when Dtx4 was overexpressed (Fig. 6 *H*). Two shRNAs
265 were designed and generated, and after validation of exogenous and endogenous
266 knockdown efficiencies, sh*dtx4*#1 was selected for the following assay (Fig. 6 *I*). Dtx4
267 knockdown remarkably abrogated CDK2 suppression of TBK1-induced IFN promoter

activity and *ifn* and *vig1* mRNAs, and CDK2 regulated both the exogenous and endogenous degradation of TBK1 (Fig. 6 *J–M*). Overall, CDK2 recruits the E3 ubiquitin ligase Dtx4 to degrade TBK1.

7. The K567 site in TBK1 plays an essential role in CDK2-mediated degradation

By accelerating CDK2-mediated TBK1 degradation, the precise ubiquitin ligase function of Dtx4 was identified. Compared to Trim11, Dtx4 significantly enhanced the CDK2-potentiated ubiquitination of TBK1 (Fig. 7 *A*). Further analysis revealed that Dtx4 overexpression augmented K48-linked TBK1 ubiquitination and that Dtx4 knockdown reduced this ubiquitination. Thus, demonstrating that Dtx4 is critical for CDK2-mediated TBK1 ubiquitination (Fig. 7 *B* and *C*). To analyze the molecular mechanism of TBK1 modification by ubiquitination, two potential TBK1 lysine sites, namely K154 and K567, were identified for modification by ubiquitination using mass spectrometry analysis (Fig. 7 *D*). Subsequently, two TBK1 mutants were generated with point mutations by mutating K154 and K567 to R to create K154R and K567R. In the ubiquitination assay, TBK1-K567R could not be ubiquitinated by CDK2, while K154R was almost identical to the wild-type TBK1 (Fig. 7 *E*). This result was also characterized in the K48-linked ubiquitination assay (Fig. 7 *F*). Moreover, Dtx4 significantly increased CDK2-mediated TBK1 wild-type and K48-linked ubiquitination but failed to enhance these processes in the K567R mutant group of TBK1 (Fig. 7 *G* and *H*). This strongly suggests that K567 is a crucial site for TBK1 ubiquitination by Dtx4. Additionally, when TBK1-K567 was mutated, CDK2-mediated degradation of TBK1 failed, and the IFN induction and antiviral capacity restriction of TBK1 by CDK2 was also ineffective (Fig. 7 *I–O*). These findings confirm the essential role of TBK1-K567 in recruiting Dtx4 through CDK2. The RING domain is crucial for E3 ubiquitin ligase activity. Three truncated mutants of Dtx4 were generated (Fig. 7 *P*). The mutant lacking the RING domain (Dtx4-△RING) significantly impaired the interaction between Dtx4 and TBK1 or CDK2 (Fig. 7 *Q*). In the ubiquitination assay, the wild-type Dtx4 enhanced TBK1 and K48-linked ubiquitination. On the other hand,

297 Dtx4-△RING failed, indicating that the RING domain was necessary for TBK1
298 ubiquitination by Dtx4 (Fig. 7 *R*). In summary, the data above demonstrates that the
299 K567 site in TBK1 and the RING domain in the E3 ubiquitin ligase Dtx4 are crucial
300 for CDK2 ubiquitination, leading to the degradation of TBK1.
301

302 **Discussion**

303 Although IFN responses exhibit powerful functions in defending against viral
304 infection, excessive activation of IFN production may cause autoimmune disease.
305 Therefore, the host needs to develop a set of regulatory mechanisms to balance immune
306 responses. In this study, we illustrated a novel role for fish CDK2 in the negative
307 regulation of IFN expression, which degraded TBK1 for K48-linked ubiquitination by
308 recruiting E3 ubiquitin ligase Dtx4.

309 TBK1 is a central kinase in MAVS, STING, and TIR-domain-containing adapter-
310 inducing IFN-β (TRIF) signaling complexes, which promote the phosphorylation of
311 IRF3 and the production of IFN. Thus, the activation of TBK1 must be tightly regulated
312 to avoid excessive autoimmune responses. TBK1 activity can be regulated in various
313 ways, including phosphorylation, ubiquitination, SUMOylation, and preventing the
314 formation of functional TBK1-containing complexes. For instance, receptor tyrosine
315 kinase HER2 recruits AKT1 to directly phosphorylate TBK1, which disrupts the
316 TBK1–STING association and K63-linked ubiquitination of TBK1, thus, suppressing
317 antiviral responses [18]. Siglec1 associates with DAP12 and SHP2 to recruit the E3
318 ubiquitin ligase TRIM27, which induces K48-linked-ubiquitination-mediated TBK1
319 degradation, resulting in the inhibition of IFN production [19]. Similar to in mammals,
320 TBK1 also dramatically activates the IFN signaling pathway in fish. Therefore, its
321 activation must be precisely modulated. For example, cytokine receptor-like factor 3
322 (Crlf3) promotes the degradation of TBK1 via K48-linked ubiquitination, resulting in
323 inhibition of IFN production [20]. While TBK1 regulation has received attention, multiple
324 molecules and underlying molecular mechanisms have not been fully characterized as
325 potential TBK1 targets.

326 Ubiquitination is one of the most versatile post-translational modifications (PTMs)
327 of proteins and plays numerous vital roles in regulating antiviral responses. Ubiquitin
328 comprises seven lysine residues (K6, K11, K27, K29, K33, K48, and K63); thus, seven
329 different polyubiquitin chains can be produced [21]. K48-linked polyubiquitination is
330 used to signal for proteasomal degradation of substrate proteins. In contrast, K63-linked
331 polyubiquitination is a non-proteolytic mode of modification that plays several vital
332 roles in stabilizing and activating target proteins [22]. Multiple studies have shown that
333 different polyubiquitin chains can regulate the expression and activation of TBK1 [5]. For
334 instance, Nrdp1, MIB1/2, RNF128, and NLRC4 mediate the K63-linked
335 polyubiquitination of TBK1 and facilitate its activation [23, 24, 25, 26]. TRIP, SOCS3, and
336 TRAF3IP3 have been proven to negatively regulate the IFN signaling pathway by
337 targeting TBK1 for K48-linked polyubiquitination and degradation [27, 28, 29].
338 Ubiquitination modification is a tightly regulated and reversible process that maintains
339 cellular homeostasis. For example, the deubiquitinating enzymes CYLD, RNF114B,
340 USP2b, and UBE2S remove the K63-linked polyubiquitination of TBK1 to block its
341 activation [30, 31, 32, 33]. Additionally, the USP1–UAF1 deubiquitinate complex has been
342 found to cleave the K48-linked polyubiquitination of TBK1 to reverse its degradation
343 process [34]. These findings are specific to the ubiquitination of mammalian TBK1.
344 Although fish TBK1 is highly conserved compared to mammalian TBK1, its
345 ubiquitination modifications are worth exploring. Our study identified a previously
346 unrecognized role for CDK2 in promoting the K48-linked polyubiquitination and
347 proteasomal degradation of fish TBK1.

348 A series of ubiquitin-related enzymes are responsible for ubiquitination,
349 including ubiquitin-activating enzymes (E1s), ubiquitin-conjugating enzymes (E2s),
350 and ubiquitin ligases (E3s). Among them, the E3s are the critical components that
351 determine the substrate specificity [35]. E3s are generally divided into two large classes,
352 including the homology to the E6-associated protein carboxyl terminus (HECT)
353 domain-containing E3 ligases and the really interesting new gene (RING) domain-
354 containing E3 ligases [36]. Multiple studies have demonstrated that E3 ligases, including
355 TRIP, Socs3, Dtx4, and TRIM27, specifically target TBK1 for K48-linked

356 polyubiquitination and degradation [19, 27, 28, 37]. However, CDK2 is not an E3 ubiquitin
357 ligase. Thus, we reasoned that CDK2 might be a mediator in the recruitment of an E3
358 ubiquitin ligase for K48-linked polyubiquitination. To validate this hypothesis, we
359 investigated and screened hTBK1-associated E3 ubiquitin ligases, demonstrating that
360 Dtx4 interacted with CDK2 and enhanced the K48-linked polyubiquitination of TBK1.
361 Meanwhile, our results showed that the RING domain in Dtx4 was necessary for
362 modifying TBK1 through ubiquitination.

363 Recent studies have demonstrated that CDK activity is crucial for virus-induced
364 innate immune responses [38]. Reports indicate that CDKs are involved in the Toll-like
365 receptor (TLR) signaling pathway, the nuclear factor-κB (NF-κB) signaling pathway,
366 and the JAK-STAT signaling pathway. For instance, CDK8 and/or CDK19 enhanced
367 the transcription of inflammatory genes, such as IL-8 and IL-10, in cells following
368 TLR9 stimulation [39]. CDKs and NF-κB establish a remarkable paradigm where CDKs
369 can act directly on substrate proteins rather than depending solely on transcriptional
370 control [40]. It has been reported that CDK1 serves as a positive regulator of the IFN-I
371 signaling pathway, facilitating STAT1 phosphorylation, which subsequently boosts the
372 expression of ISGs [41]. Furthermore, inhibiting CDK activity has been shown to obstruct
373 STAT phosphorylation, proinflammatory gene activation, and ISG mRNA induction in
374 response to SeV infection [42]. It is important to note that no evidence suggests the
375 involvement of CDKs in RLR signaling pathways. This study has shown that fish
376 CDK2 functions as a negative regulator of the key kinase TBK1, which is involved in
377 the RLR signaling pathway. Variations in CDK2 activity during different phases of the
378 cell cycle may lead to changes in the expression and function of TBK1. Our findings
379 suggest that heightened CDK2 activity may suppress TBK1 expression, thereby
380 hindering the cell's capacity to produce IFN. Conversely, during the late phase of the
381 cell cycle or in an inhibited state, TBK1 expression may rise, enhancing IFN synthesis
382 and release. In summary, CDK2 is involved in intracellular signaling by modulating
383 TBK1 levels and IFN production, affecting the cellular immune response and cycle
384 regulation—two processes that are notably distinct at various stages of the cell cycle.
385 A better understanding of the relationship between CDK2 and RLR signaling pathways

386 will enhance our grasp of the regulatory mechanisms of CDKs in antiviral innate
387 immunity.

388 CDK2 is a multifunctional kinase involved in many critical cellular processes,
389 including cell cycle progression, differentiation, cancer, immunity, etc. [43]. To date, there
390 has been limited research conducted on fish CDK2 in the regulation of cell cycle
391 progression. The details are as follows: It has been reported that the kinase activity of
392 goldfish CDK2 significantly increases during oocyte maturation [44]. Furthermore,
393 UHRF1 phosphorylation by cyclin A2/CDK2 is crucial for zebrafish embryogenesis [45].
394 Additionally, a novel CDK2 homolog has been identified in Japanese lamprey, which
395 plays a crucial role in apoptosis [46]. Red grouper nervous necrosis virus (RGNNV)
396 infection activates the p53 pathway, leading to the upregulation of p21 and
397 downregulation of cyclin E and CDK2, which forces infected cells to remain in the
398 G1/S replicative phase [47]. In addition, we selected representative species from each of
399 the six major vertebrate groups and compared their CDK2 protein sequences,
400 discovering that they are over 90% similar to one another. This suggests that the
401 function of CDK2 may be conserved to some extent across vertebrates. Furthermore,
402 CDK2 inhibition has been shown to enhance anti-tumor immunity by increasing the
403 IFN response to endogenous retroviruses [12]. Here, we reveal the role of CDK2 in
404 modulating the RLR signaling pathway during innate immunity. Upon infection with
405 SVCV, CDK2 expression was induced. CDK2 deficiency or knockdown enhanced the
406 antiviral response both *in vitro* and *in vivo*, while CDK2 overexpression promoted viral
407 replication. Thus, our study identifies CDK2 as a negative regulator of antiviral immune
408 responses in addition to its well-studied function in cell cycle regulation. Meanwhile,
409 the E3 ubiquitin ligase Dtx4 is also required to regulate antiviral immune responses.
410 Further studies are needed to determine how CDK2 regulates Dtx4 activation and the
411 detailed mechanisms involved.

412 In conclusion, our results identified a novel function of CDK2 in the negative
413 regulation of TBK1-mediated IFN production. CDK2 interacted with TBK1 and
414 recruited the E3 ubiquitin ligase Dtx4 to facilitate the K48-linked polyubiquitination at
415 Lys567 residues in TBK1, eventually leading to the proteasomal degradation of TBK1.

416 Our findings have revealed a previously unrecognized role for CDK2 in regulating
417 immune homeostasis, providing molecular insight into the mechanisms through which
418 CDK2–DTX4 targets TBK1 for ubiquitination and degradation.
419

420 # Methods

421 **Ethics statement**

422 The experiments involved in this study were conducted in compliance with ethical
423 regulations. The fish experiments were carried out under the guidance of the European
424 Union Guidelines for the Handling of Laboratory Animals (2010/63/EU) and approved
425 by the Ethics Committee for Animal Experiments of the Institute of Aquatic Biology
426 of the Chinese Academy of Sciences (No. 2023-068).

427 **Fish, cells, and viruses**

428 Mature zebrafish individuals 2.5 months after hatching (0.4 ± 0.1 g) were selected
429 in this study. AB line wild-type zebrafish (Danio rerio) and cdk2 mutant zebrafish
430 (CZ1442: *cdk2*$^{ihb488/+}$) were obtained from the China National Zebrafish Resource
431 Center (CZRC) and bred using standardized procedures. In accordance with ethical
432 requirements and national animal welfare guidelines, all experimental fish were
433 required to undergo a two-week acclimatization period in the laboratory and have their
434 health assessed prior to the study. Only fish that appeared healthy and were mobile were
435 used for scientific research. ZF4 cells (American Type Culture Collection, ATCC) were
436 cultured in Ham's F-12 medium (Invitrogen) supplemented with 10% fetal bovine
437 serum (FBS) at 28 ˚C and 5% CO_2. EPC cells and ctenopharyngodon idellus kidney
438 (CIK) cells were obtained from the Chinese Culture Collection Centre for Type
439 Cultures (CCTCC), Gibel carp brain (GiCB) cells were provided by Ling-Bing Zeng
440 (Yangtze River Fisheries Research Institute, Chinese Academy of Fishery Sciences),
441 these cells were maintained at 28°C in 5% CO_2 in medium 199 (Invitrogen)
442 supplemented with 10% FBS. THP1 cells originally obtained from ATCC were
443 maintained in RPMI 1640 medium supplemented with 10% FBS. SVCV was
444 propagated in EPC cells until a cytopathogenic effect (CPE) was observed, and then

445 cell culture fluid containing SVCV was harvested and centrifuged at 4×10^3 *g* for 20
446 min to remove the cell debris, and the supernatant was stored at -80°C until used. GCRV
447 (strain 873, group I) and vesicular stomatitis virus (VSV) was provided by Prof. Wuhan
448 Xiao (Institute of Hydrobiology, Chinese Academy of Sciences). GCRV was
449 propagated in CIK cells and harvested in a similar way to SVCV. Cyprinid herpesvirus
450 2 (CyHV2, obtained from Yancheng city, Jiangsu province, China) was provided by
451 Prof. Liqun Lu (Shanghai Ocean University). CyHV-2 was propagated in GICB cells
452 and harvested in a similar way to SVCV.

453 **Plasmid construction and reagents**

454 The sequence of zebrafish CDK2 (GenBank accession number: NM_213406.1)
455 was obtained from the National Centre for Biotechnology Information (NCBI) website.
456 CDK2 was amplified by polymerase chain reaction (PCR) using cDNA from adult
457 zebrafish tissues as a template and cloned into the expression vector pCMV-HA or
458 pCMV-Myc (Clontech) vectors. Zebrafish MAVS (NM_001080584.2), TBK1
459 (NM_001044748.2) and the truncated mutants of TBK1, Dtx4 (XM_002660524.5) and
460 the truncated mutants of Dtx4, Trim11 (XM_021470074.1), Traip (NM_205607.1),
461 Socs3a (NM_199950.1), and GAPDH (NM_001115114.1) were cloned into pCMV-
462 Myc and pCMV-Tag2C vectors. The short hairpin RNA of Pimephales promelas CDK2
463 (XM_039663387.1) and Dtx4 (XM_039689084.1) were designed by BLOCK-iT RNAi
464 Designer and cloned into the pLKO.1-TRC Cloning vector. For subcellular localization
465 experiments, CDK2 was constructed onto pEGFP-N3 (Clontech), while MAVS and
466 TBK1 were constructed onto pCS2-mCherry (Clontech). The plasmids containing
467 zebrafish IFNφ1pro-Luc and ISRE-Luc in the pGL3-Basic luciferase reporter vector
468 (Promega) were constructed as described previously. The *Renilla* luciferase internal
469 control vector (pRL-TK) was purchased from Promega. The ubiquitin mutant
470 expression plasmids Lys-48 and Lys-63 (all lysine residues were mutated except Lys-
471 48 or Lys-63) were ligated into the pCMV-HA vectors named Ub-K48O-HA and Ub-
472 K63O-HA. All constructs were confirmed by DNA sequencing. Polyinosinic-
473 polycytidylic acid (poly I:C) was purchased from Sigma-Aldrich used at a final
474 concentration of 1 μg/μl. MG132 (Cat. No. M7449), 3-Methyladenine (3-MA) (Cat.

475 No. M9281), Chloroquine (CQ) (Cat. No. C6628) were obtained from Sigma-Aldrich.
476 Bafilomycin A1 (Baf-A1) (Cat. No. S1413) was obtained from Selleck.

477 **Transcriptomic analysis**

478 Total RNA was extracted using the TRIzol method and assessed for RNA purity
479 and quantification using a NanoDrop 2000 spectrophotometer (Thermo Scientific,
480 Waltham, U.S.A.), and RNA integrity was assessed using an Agilent 2100 Bioanalyzer
481 (Agilent Technologies, Santa Clara, U.S.A.). Santa Clara, U.S.A). Transcriptome
482 sequencing and data analysis were performed by OE Biotech (Shanghai, China). The
483 raw sequencing data was submitted to the NGDC (National Genomics Data Center)
484 (GSA accession number: CRA008409).

485 **Transient transfection and virus infection**

486 EPC cells were transfected in 6-well and 24-well plates using transfection reagents
487 from FishTrans (MeiSenTe Biotechnology) according to the manufacturer's protocol.
488 Antiviral assays were performed in 24-well plates by transfecting EPC cells with the
489 plasmids shown in the figure. At 24 h post-transfection, cells were infected with SVCV
490 at a multiplicity of infection (MOI = 0.001), GCRV (MOI = 0.001), CyHV-2 (MOI =
491 0.1). After 48 h or 72 h, supernatant aliquots were harvested for detection of virus titers,
492 the cell monolayers were fixed by 4% paraformaldehyde (PFA) and stained with 1%
493 crystal violet for visualizing CPE. For virus titration, 200 μl of culture medium were
494 collected at 48 h post-infection and used for detection of virus titers according to the
495 method of Reed and Muench. The supernatants were subjected to 3-fold or 10-fold
496 serial dilutions and then added (100 μl) onto a monolayer of EPC cells cultured in a 96-
497 well plate. After 48 or 72 h, the medium was removed and the cells were washed with
498 PBS, fixed by 4% PFA and stained with 1% crystal violet. The virus titer was expressed
499 as 50% tissue culture infective dose ($TCID_{50}$/ml). For viral infection, fish were
500 anesthetized with methanesulfonate (MS-222) and intraperitoneally (i.p.) injected with
501 5 μl of M199 containing SVCV (5×10^8 $TCID_{50}$/ml). The i.p. injection of PBS was
502 used as mock infection. Then the fish were migrated into the aquarium containing new
503 aquatic water.

504 **Luciferase activity assay**

505 EPC cells were cultured overnight in 24-well plates and then co-transfected with
506 the expression plasmid and luciferase reporter plasmid. The cells were infected with
507 SVCV or transfected with poly I:C for 24 h prior to harvest. To ensure that the same
508 total amount of DNA was transfected in each well, pCMV-HA empty vector was used.
509 At 24 h post-stimulation, cells were washed with phosphate-buffered saline (PBS) and
510 lysed for measuring luciferase activity by the Dual-Luciferase Reporter Assay System
511 (Promega) according to the manufacturer's instructions. Firefly luciferase activity was
512 normalized based on the Renilla luciferase activity.

513 **RNA extraction, reverse transcription, and quantitative PCR (qPCR)**

514 The RNA was extracted using TRIzol reagent (Invitrogen), and first-strand cDNA
515 was synthesized with a PrimeScript RT kit with gDNA Eraser (Takara). qPCR was
516 performed on the CFX96 Real-Time System (Bio-Rad) using SYBR green PCR Master
517 Mix (Yeasen). PCR conditions were as follows: 95°C for 5 min and then 40 cycles of
518 95°C for 20 s, 60°C for 20 s, and 72°C for 20 s. All primers used for qPCRs are shown
519 in Table S1, and *β-actin* gene was used as an internal control. The relative fold changes
520 were calculated by comparison to the corresponding controls using the $2^{-\Delta\Delta Ct}$ method
521 (where CT was the threshold cycle).

522 **Co-immunoprecipitation (Co-IP) assay**

523 EPC cells were cultured in 10 cm^2 dishes overnight and transfected with 10 μg of
524 plasmid, as shown. At 24 h post-transfection, the medium was discarded, and the cells
525 were washed with PBS. Then the cells were lysed in 1 ml of radioimmunoprecipitation
526 (RIPA) lysis buffer [1% NP-40, 50 mM Tris-HCl, pH 7.5, 150 mM NaCl, 1 mM EDTA,
527 1 mM NaF, 1 mM sodium orthovanadate (Na_3VO_4), 1 mM phenyl-methylsulfonyl
528 fluoride (PMSF), 0.25% sodium deoxycholate] containing protease inhibitor cocktail
529 (Sigma-Aldrich) at 4°C for 1 h on a rocker platform. The cellular debris was removed
530 by centrifugation at 12,000 × *g* for 15 min at 4°C. The supernatant was transferred to a
531 fresh tube and incubated with 20 μl anti-Flag/HA/Myc affinity gel (Sigma-Aldrich)
532 overnight at 4°C with constant rotating incubation. These samples were further
533 analyzed by immunoblotting (IB). Immunoprecipitated proteins were collected by
534 centrifugation at 5000 × *g* for 1 min at 4°C, washed three times with lysis buffer and

535 resuspended in 50 μl 2 × SDS sample buffer. The immunoprecipitates and whole cell
536 lysates (WCLs) were analyzed by IB with the indicated antibodies (Abs).

537 **In vivo ubiquitination assay**

538 Transfected EPC cells were washed twice with 10 mL ice-cold PBS and then
539 digested with 1 mL 0.25% trypsin-EDTA (1×) (Invitrogen) for 2–3 min until the cells
540 were dislodged. 100 μL FBS was added to neutralize the trypsin and the cells were
541 resuspended into 1.5 mL centrifuge tube, centrifuged at 2000 ×*g* for 5 min. The
542 supernatant was discarded and the cell precipitations were resuspended using 1 mL PBS
543 and centrifuged at 2000 ×*g* for 5 min. The collected cell precipitations were lysed using
544 100 μL PBS containing 1% SDS and denatured by heating for 10 min. The supernatants
545 were diluted with lysis buffer until the concentration of SDS was decreased to 0.1%.
546 The diluted supernatants were incubated with 20 μL anti-Myc affinity gel overnight at
547 4°C with constant agitation. These samples were further analyzed by IB.
548 Immunoprecipitated proteins were collected by centrifugation at 5000 ×*g* for 1 min at
549 4°C, washed for three times with lysis buffer and resuspended in 100 μL 1× SDS sample
550 buffer.

551 **Immunoblot analysis**

552 Immunoprecipitates or WCLs were analyzed as described previously. Antibodies
553 were diluted as follows: anti-β-actin (ABclonal, AC026) at 1:3000, anti-Flag (Sigma-
554 Aldrich, F1804) at 1:3000, anti-HA (Covance, MMS-101R) at 1:3000, anti-Myc (Santa
555 Cruz Biotechnology, sc-40) at 1:3000, anti-Dtx4 (Thermo Scientific, PA5-46146) at
556 1:1000, anti-CDK2 (GeneTex, GTX101226) at 1:1000, and HRP-conjugated anti-
557 mouse/rabbit IgG (Thermo Scientific, 31430/31460) at 1:5000, anti-
558 N/P/G/TBK1/CDK2 (prepared and purified in our lab) at 1:2000.

559 **Immunofluorescence (IF)**

560 EPC cells were plated onto glass coverslips in 6-well plates and infected with
561 SVCV (MOI = 1) 24 h. Then the cells were washed with PBS and fixed in 4% PFA at
562 room temperature for 1 h and permeabilized with 0.2% Triton X-100 in ice-cold PBS
563 for 15 min. The samples were blocked for 1 h at room temperature in PBS containing
564 2% bovine serum albumin (BSA, Sigma-Aldrich). After additional PBS washing, the

samples were incubated with anti-N Ab in PBS containing 2% BSA for 2-4 h at room temperature. After three times washed by PBS, the samples were incubated with secondary Ab (Alexa Fluor 488 AffiniPure Donkey anti-Rabbit IgG (H+L) (34206ES60, 1:10,000) in PBS containing 2% BSA for 1 h at room temperature. After additional PBS washing, the cells were finally stained with 1 μg/ml 4′, 6-diamidino-2-phenylindole (DAPI; Beyotime Institute of Biotechnology, Shanghai, China) for 10 min in the dark at room temperature. Finally, the coverslips were washed and observed with a confocal microscope under a 10× immersion objective (SP8; Leica).

Fluorescent microscopy

EPC cells were plated onto coverslips in 6-well plates and transfected with the plasmids indicated for 24 h. Then the cells were washed twice with PBS and fixed with 4% PFA for 1 h. After being washed three times with PBS, the cells were stained with 1 μg/ml DAPI for 15 min in the dark at room temperature. Finally, the coverslips were washed and observed with a confocal microscope under a 63× oil immersion objective (SP8; Leica).

Histopathology

Liver, spleen, and kidney tissues from three individuals of control or virus-infected fish at 2 days post infection (dpi) were dissected, and fixed in 10% phosphate-buffered formalin overnight. Then the samples were dehydrated in ascending grades of alcohol and embedded into paraffin. Sections at 5 μm thickness were taken and stained with hematoxylin and eosin (H&E). Histological changes were examined by optical microscopy at ×40 magnification and were analyzed by the Aperio ImageScope software.

Statistics analysis

For fish survival analysis, Kaplan-Meier survival curves were generated and analyzed by Log-rank test. For the bar graph, one representative experiment of at least three independent experiments is shown, and each was done in triplicate. For the dot plot graph, each dot point represents one independent biological replicate. Unpaired Student's t test was used for statistical analysis. Data are expressed as mean ± standard error of the mean (SEM). A p value < 0.05 was considered statistically significant.

Acknowledgments

We thank Fang Zhou (Institute of Hydrobiology, Chinese Academy of Sciences) for assistance with confocal microscopy analysis and Dr. Feng Xiong (China Zebrafish Resource Center, Institute of Hydrobiology, Chinese Academy of Sciences) for assistance with qPCR analysis.

This work was supported by the Strategic Priority Research Program of the Chinese Academy of Sciences (XDB0730300), National Excellent Youth Science Fund (32322086), National Natural Science Foundation of China (32073009), and the Youth Innovation Promotion Association provided funding to Shun Li. National Key Research and Development Program of China (2023YFD2400201) provided funding to Dan-Dan Chen. National Natural Science Foundation of China (32173023) provided funding to Long-Feng Lu.

Author Contributions

L.F.L. and S.L. conceptualized the study and wrote the original draft. L.F.L. did data analysis. C.Z., Z.C.L., and B.J.C. were responsible for sample collection. D.D.C., S.L., and L.F.L. are responsible for funding resources. All authors reviewed and edited the manuscript. All authors had full access to all the data in the study and had final responsibility for the decision to submit for publication.

Declaration of interests

The authors declare no competing interests.

References:

1. Kisseleva T, Bhattacharya S, Braunstein J, Schindler CW. Signaling through the JAK/STAT pathway, recent advances and future challenges. *Gene* **285**, 1-24 (2002).

2. Sadler AJ, Williams BRG. Interferon-inducible antiviral effectors. *Nat Rev Immunol* **8**, 559-568 (2008).

3. Kumar H, Kawai T, Akira S. Pathogen recognition by the innate immune system. *Int Rev*

Immunol **30**, 16-34 (2011).

4. Fitzgerald KA, *et al.* IKKepsilon and TBK1 are essential components of the IRF3 signaling pathway. *Nat Immunol* **4**, 491-496 (2003).

5. Zhao W. Negative regulation of TBK1-mediated antiviral immunity. *FEBS letters* **587**, 542-548 (2013).

6. Cui J, *et al.* NLRP4 negatively regulates type I interferon signaling by targeting the kinase TBK1 for degradation via the ubiquitin ligase DTX4. *Nature immunology* **13**, 387-395 (2012).

7. Cui J, *et al.* NLRP4 negatively regulates type I interferon signaling by targeting the kinase TBK1 for degradation via the ubiquitin ligase DTX4. *Nat Immunol* **13**, 387-395 (2012).

8. An T, *et al.* DYRK2 Negatively Regulates Type I Interferon Induction by Promoting TBK1 Degradation via Ser527 Phosphorylation. *PLoS pathogens* **11**, e1005179 (2015).

9. Lu LF, *et al.* A novel role of Zebrafish TMEM33 in negative regulation of interferon production by two distinct mechanisms. *PLoS pathogens* **17**, e1009317 (2021).

10. Fagundes R, Teixeira LK. Cyclin E/CDK2: DNA Replication, Replication Stress and Genomic Instability. *Front Cell Dev Biol* **9**, (2021).

11. Schmitz ML, Kracht M. Cyclin-Dependent Kinases as Coregulators of Inflammatory Gene Expression. *Trends Pharmacol Sci* **37**, 101-113 (2016).

12. Chen Y, *et al.* CDK2 Inhibition Enhances Antitumor Immunity by Increasing IFN Response to Endogenous Retroviruses. *Cancer Immunol Res* **10**, 525-539 (2022).

13. Cingoz O, Goff SP. Cyclin-dependent kinase activity is required for type I interferon production. *Proc Natl Acad Sci U S A* **115**, E2950-E2959 (2018).

14. Sun F, *et al.* Characterization of fish IRF3 as an IFN-Iinducible protein reveals evolving regulation of IFN response in vertebrates. *J Immunol* **185**, 7573-7582 (2010).

15. Panne D, McWhirter SM, Maniatis T, Harrison SC. Interferon regulatory factor 3 is regulated by a dual phosphorylation-dependent switch. *J Biol Chem* **282**, 22816-22822 (2007).

16. Li S, *et al.* Zebrafish MVP Recruits and Degrades TBK1 To Suppress IFN Production. *The Journal of Immunology* **202**, 559-566 (2019).

17. Liu S, *et al.* Major vault protein: A virus-induced host factor against viral replication through the induction of type-I interferon. *Hepatology* **56**, 57-66 (2012).

670 18. Wu SY, *et al.* HER2 recruits AKT1 to disrupt STING signalling and suppress antiviral defence
671 and antitumour immunity. *Nature cell biology* **21**, 1027-+ (2019).
672
673 19. Zheng Q, Hou J, Zhou Y, Yang Y, Xie B, Cao X. Siglec1 suppresses antiviral innate immune
674 response by inducing TBK1 degradation via the ubiquitin ligase TRIM27. *Cell research* **25**,
675 1121-1136 (2015).
676
677 20. Yan XL, Zheng WW, Geng S, Zhou M, Xu TJ. Cytokine Receptor-Like Factor 3 Negatively
678 Regulates Antiviral Immunity by Promoting the Degradation of TBK1 in Teleost Fish. *Journal*
679 *of virology* **97**, (2023).
680
681 21. Song L, Luo ZQ. Post-translational regulation of ubiquitin signaling. *The Journal of cell biology*
682 **218**, 1776-1786 (2019).
683
684 22. Kulathu Y, Komander D. Atypical ubiquitylation - the unexplored world of polyubiquitin
685 beyond Lys48 and Lys63 linkages. *Nat Rev Mol Cell Biol* **13**, 508-523 (2012).
686
687 23. Wang C, *et al.* The E3 ubiquitin ligase Nrdp1 'preferentially' promotes TLR-mediated
688 production of type I interferon. *Nature immunology* **10**, 744-752 (2009).
689
690 24. Ye JS, Kim N, Lee KJ, Nam YR, Lee U, Joo CH. Lysine 63-Linked TANK-Binding Kinase 1
691 Ubiquitination by Mindbomb E3 Ubiquitin Protein Ligase 2 Is Mediated by the Mitochondrial
692 Antiviral Signaling Protein. *Journal of virology* **88**, 12765-12776 (2014).
693
694 25. Song GH, *et al.* E3 ubiquitin ligase RNF128 promotes innate antiviral immunity through K63-
695 linked ubiquitination of TBK1. *Nature immunology* **17**, 1342-1351 (2016).
696
697 26. Zhang R, Yang W, Zhu H, Jingbo Z, Xue M, Zheng C. NLRC4 promotes the cGAS-STING
698 signaling pathway by facilitating CBL-mediated K63-linked polyubiquitination of TBK1.
699 *Journal of medical virology* **95**, e29013 (2023).
700
701 27. Zhang M, *et al.* TRAF-interacting protein (TRIP) negatively regulates IFN-beta production and
702 antiviral response by promoting proteasomal degradation of TANK-binding kinase 1. *The*
703 *Journal of experimental medicine* **209**, 1703-1711 (2012).
704
705 28. Liu D, *et al.* SOCS3 Drives Proteasomal Degradation of TBK1 and Negatively Regulates
706 Antiviral Innate Immunity. *Molecular and cellular biology* **35**, 2400-2413 (2015).
707
708 29. Deng M, *et al.* TRAF3IP3 negatively regulates cytosolic RNA induced anti-viral signaling by
709 promoting TBK1 K48 ubiquitination. *Nat Commun* **11**, 2193 (2020).
710
711 30. Friedman CS, *et al.* The tumour suppressor CYLD is a negative regulator of RIG-I-mediated
712 antiviral response. *EMBO reports* **9**, 930-936 (2008).
713

31. Zhang Z, *et al.* RNF144B inhibits LPS-induced inflammatory responses via binding TBK1. *J Leukoc Biol* **106**, 1303-1311 (2019).

32. Zhang L, Zhao X, Zhang M, Zhao W, Gao C. Ubiquitin-specific protease 2b negatively regulates IFN-beta production and antiviral activity by targeting TANK-binding kinase 1. *Journal of immunology* **193**, 2230-2237 (2014).

33. Huang L, *et al.* Ubiquitin-Conjugating Enzyme 2S Enhances Viral Replication by Inhibiting Type I IFN Production through Recruiting USP15 to Deubiquitinate TBK1. *Cell reports* **32**, (2020).

34. Yu Z, *et al.* USP1–UAF1 deubiquitinase complex stabilizes TBK1 and enhances antiviral responses. *The Journal of experimental medicine* **214**, jem.20170180 (2017).

35. Pickart CM. Mechanisms underlying ubiquitination. *Annu Rev Biochem* **70**, 503-533 (2001).

36. Metzger MB, Hristova VA, Weissman AM. HECT and RING finger families of E3 ubiquitin ligases at a glance. *Journal of cell science* **125**, 531-537 (2012).

37. Cui J, *et al.* NLRP4 negatively regulates type I interferon signaling by targeting the kinase TBK1 for degradation via the ubiquitin ligase DTX4. *Nature immunology* **13**, 387-395 (2012).

38. Zheng CF, Tang YD. The emerging roles of the CDK/cyclin complexes in antiviral innate immunity. *Journal of Medical Virology* **94**, 2384-2387 (2022).

39. Yamamoto S, *et al.* Mediator cyclin-dependent kinases upregulate transcription of inflammatory genes in cooperation with NF-B and C/EBP on stimulation of Toll-like receptor 9. *Genes Cells* **22**, 265-276 (2017).

40. Perkins ND, Felzien LK, Betts JC, Leung KY, Beach DH, Nabel GJ. Regulation of NF-kappa B by cyclin-dependent kinases associated with the p300 coactivator. *Science* **275**, 523-527 (1997).

41. Wu LL, *et al.* Identification of Cyclin-Dependent Kinase 1 as a Novel Regulator of Type I Interferon Signaling in Systemic Lupus Erythematosus. *Arthritis Rheumatol* **68**, 1222-1232 (2016).

42. Cingöz O, Goff SP. Cyclin-dependent kinase activity is required for type I interferon production. *P Natl Acad Sci USA* **115**, E2950-E2959 (2018).

43. Tadesse S, *et al.* Targeting CDK2 in cancer: challenges and opportunities for therapy. *Drug Discov Today* **25**, 406-413 (2020).

44. Hirai T, *et al.* Isolation and Characterization of Goldfish Cdk2, a Cognate Variant of the Cell-

Cycle Regulator Cdc2. *Developmental biology* **152**, 113-120 (1992).

45. Chu J, *et al.* UHRF1 phosphorylation by cyclin A2/cyclin-dependent kinase 2 is required for zebrafish embryogenesis. *Molecular biology of the cell* **23**, 59-70 (2012).

46. Xu Y, Tian Y, Zhao H, Zheng N, Ren KX, Li QW. A novel CDK-2 homolog identified in lamprey, with roles in apoptosis. *Fish Physiol Biochem* **47**, 189-189 (2021).

47. Mai WJ, Liu HX, Chen HQ, Zhou YJ, Chen Y. RGNNV-induced cell cycle arrest at G1/S phase enhanced viral replication via p53-dependent pathway in GS cells. *Virus Res* **256**, 142-152 (2018).

Figure Legends

Figure 1. *In vivo and in vitro*, CDK2 is upregulated during viral infection. (A) Schematic representation of zebrafish tissue dissection and RNA extraction for transcriptome sequencing. The liver and spleen tissues from male and female zebrafish injected with PBS (5 μL/individual), SVCV (5×10^8 $TCID_{50}$/mL, 5 μL/individual) for 48 h. Total RNAs were extracted and used for transcriptome sequencing and analysis. (B) Heatmap view of mRNA variations of CDKs in the liver and spleen of zebrafish with or without SVCV infection. (C) qPCR analysis of *cdk2* mRNA in the THP-1, GICB, ZF4, or EPC cells infected with VSV, CyHV-2, or SVCV for the indicated times. (D) qPCR analysis of *cdk2* mRNA in the liver and spleen of zebrafish (n = 5 per group) given injected intraperitoneally (i.p.) with PBS or SVCV for 48 h. (E) IB of proteins in the liver and spleen of zebrafish (n = 3 per group) given i.p. injection of PBS or SVCV for 48 h. (F) IB of proteins in ZF4 and EPC cells infected with SVCV for the indicated times.

Figure 2. CDK2 deficiency protects fish from SVCV infection. (A) Survival (Kaplan-Meier Curve) of $cdk2^{+/+}$ and $cdk2^{-/-}$ zebrafish (n = 15 per group) at various days after i.p. infected with SVCV (5×10^8 $TCID_{50}$/mL, 5 μL/individual). (B) Microscopy of H&E-stained liver, spleen, and kidney sections from $cdk2^{+/+}$ and $cdk2^{-/-}$ zebrafish treated with SVCV for 48 h. (C) qPCR analysis of *svcv-n* mRNA in the liver,

791 spleen, and kidney of *cdk2*$^{+/+}$ and *cdk2*$^{-/-}$ zebrafish (n = 6 per group) given i.p. injection
792 of SVCV for 48 h. (D) IB of proteins in the liver, spleen, and kidney sections from
793 *cdk2*$^{+/+}$ and *cdk2*$^{-/-}$ zebrafish (n = 3 per group) treated with SVCV for 48 h. (E) CDK2
794 regulates antiviral response-relevant target genes, presented as a volcano plot of genes
795 with differential expression after SVCV infection in the liver of *cdk2*$^{+/+}$ and *cdk2*$^{-/-}$
796 zebrafish. (F) GSEA of differentially expressed genes in the liver of *cdk2*$^{+/+}$ and *cdk2*$^{-/-}$
797 zebrafish with SVCV infection and enrichment of IFN. FDR (*q*-value) was shown. (G)
798 Heatmap view of mRNA variations of IFN-mediated ISG sets in the liver of *cdk2*$^{+/+}$ and
799 *cdk2*$^{-/-}$ zebrafish with SVCV infection. (H) qPCR analysis of *ifnφ1* mRNA in the liver,
800 spleen, and kidney of *cdk2*$^{+/+}$ and *cdk2*$^{-/-}$ zebrafish (n = 6 per group) given i.p. injection
801 of SVCV for 48 h.

802 **Figure 3. CDK2 negatively regulates IFN production and promotes viral**
803 **replication.** (A and C) Luciferase activity of IFNφ1pro and ISRE in EPC cells
804 transfected with indicated plasmids for 24 h, and then untreated or infected with SVCV
805 (MOI = 1) or transfected with poly I:C (0.5 μg) for 24 h before luciferase assays. (B)
806 IB of proteins in EPC cells transfected with indicated plasmids for 24 h. (D) qPCR
807 analysis of *ifn* and *vig1* in EPC cells transfected with indicated plasmids for 24 h, and
808 then untreated or infected with SVCV (MOI = 1) or transfected with poly I:C (2 μg) for
809 24 h. (E and F) Plaque assay of virus titers in EPC, CIK, and GiCB cells transfected
810 with indicated plasmids for 24 h, followed by SVCV, GCRV, and CyHV-2 challenge
811 for 24-72 h. (G and H) qPCR and IB analysis of SVCV genes in EPC cells transfected
812 with indicated plasmids for 24 h, followed by SVCV challenge for 24 h. (I) IF analysis
813 of N protein in EPC cells transfected with indicated plasmids for 24 h, followed by
814 SVCV challenge for 24 h. The fluorescence intensity (arbitrary unit, a.u.) was recorded
815 by the LAS X software, and the data were expressed as mean ± SD, n = 5.

816 **Figure 4. CDK2 associates with TBK1 and mediates its degradation.** (A and B)
817 Luciferase activity of IFNφ1pro and ISRE in EPC cells transfected with indicated
818 plasmids for 24 h. (C and D) qPCR analysis of *ifn* and *vig1* in EPC cells transfected
819 with indicated plasmids for 24 h. (E) Confocal microscopy of CDK2 and TBK1 in EPC
820 cells transfected with indicated plasmids for 24 h. The coefficient of colocalization was

821 determined by qualitative analysis of the fluorescence intensity of the selected area in
822 Merge. (F) IB of WCLs and proteins immunoprecipitated with anti-Myc antibody-
823 conjugated agarose beads from EPC cells transfected with indicated plasmids for 24 h.
824 (G) IB of WCLs and proteins immunoprecipitated with anti-TBK1 or anti-CDK2
825 antibody from EPC cells infected with SVCV for 24 h. (H) Schematic representation of
826 full-length TBK1 and its mutants. (I) IB of WCLs and proteins immunoprecipitated
827 with anti-Flag antibody-conjugated agarose beads from EPC cells transfected with
828 indicated plasmids for 24 h. (J) IB of proteins in EPC cells transfected with indicated
829 plasmids for 24 h. (K and L) IB of proteins in EPC cells transfected with CDK2-HA or
830 sh*cdk2*#1 for 24 h, followed by untreated or infected with SVCV (MOI = 1) or
831 transfected with poly I:C (2 μg) for 24 h. (M) IB of proteins in the liver, spleen, and
832 kidney sections from *cdk2*$^{+/+}$ and *cdk2*$^{-/-}$ zebrafish (n = 3 per group). (N) Plaque assay
833 of virus titers in EPC cells transfected with indicated plasmids for 24 h, followed by
834 SVCV challenge for 24-48 h. (O and Q) IB and qPCR analysis of SVCV genes in EPC
835 cells transfected with indicated plasmids for 24 h, followed by SVCV challenge for 24
836 h. (P) IF analysis of N protein in EPC cells transfected with indicated plasmids for 24
837 h, followed by SVCV challenge for 24 h. The fluorescence intensity (arbitrary unit, a.u.)
838 was recorded by the LAS X software, and the data were expressed as mean ± SD, n =
839 5.

840 **Figure 5. CDK2 increases the K48-linked polyubiquitination of TBK1.** (A) qPCR
841 analysis of *epc-tbk1* in EPC cells transfected with indicated plasmids for 24 h, and then
842 untreated or infected with SVCV (MOI = 1) or transfected with poly I:C (2 μg) for 24
843 h. (B and C) IB of proteins in EPC cells transfected with indicated plasmids for 18 h,
844 followed by treatments of MG132 (10 μM), 3-MA (2 mM), Baf-A1 (100 nM), and CQ
845 (50 μM) for 6 h, respectively. (D) IB of proteins in EPC cells transfected with CDK2-
846 HA for 24 h, followed by untreated or infected with SVCV (MOI = 1) or transfected
847 with poly I:C (2 μg) for 24 h. Protein lysates were harvested after MG132 (20 μM)
848 treatments (6 h) for IB analysis. (E) TBK1 ubiquitination assays in EPC cells
849 transfected with indicated plasmids for 18 h, followed by DMSO or MG132 treatments
850 for 6 h. (F) Mass spectrometry analysis of a peptide derived from ubiquitinated TBK1-

851 Myc. (G and H) TBK1 ubiquitination assays in EPC cells transfected with indicated
852 plasmids for 18 h, followed by MG132 treatments for 6 h.
853 **Figure 6. CDK2 recruits Dtx4 to degrade TBK1.** (A-D) IB of WCLs and proteins
854 immunoprecipitated with anti-Myc or Flag Ab-conjugated agarose beads from EPC
855 cells transfected with indicated plasmids for 24 h. (E and J) Luciferase activity of
856 IFNφ1pro in EPC cells transfected with indicated plasmids for 24 h. (F and K) qPCR
857 analysis of *ifn* and *vig1* in EPC cells transfected with indicated plasmids for 24 h. (G
858 and L) IB of proteins in EPC cells transfected with indicated plasmids for 24 h. (H and
859 M) IB of proteins in EPC cells transfected with CDK2-HA and Dtx4-Myc or sh*dtx4*#1
860 for 24 h, followed by untreated or infected with SVCV (MOI = 1) or transfected with
861 poly I:C (2 μg) for 24 h.
862 **Figure 7. K567 site is critical for the ubiquitination degradation of TBK1.** (A-C)
863 TBK1 ubiquitination assays in EPC cells transfected with indicated plasmids for 18 h,
864 followed by MG132 treatments for 6 h. (D) Mass spectrometry analysis to show that
865 K154 and K567 of TBK1 is conjugated with ubiquitin. (E-H) TBK1 ubiquitination
866 assays in EPC cells transfected with indicated plasmids for 18 h, followed by MG132
867 treatments for 6 h. (I) IB of proteins in EPC cells transfected with indicated plasmids
868 for 24 h. (J) Luciferase activity of IFNφ1pro in EPC cells transfected with indicated
869 plasmids for 24 h. (K) qPCR analysis of *ifn* in EPC cells transfected with indicated
870 plasmids for 24 h. (L) Plaque assay of virus titers in EPC cells transfected with indicated
871 plasmids for 24 h, followed by SVCV challenge for 24-48 h. (M and N) qPCR and IB
872 analysis of SVCV genes in EPC cells transfected with indicated plasmids for 24 h,
873 followed by SVCV challenge for 24 h. (O) IF analysis of N protein in EPC cells
874 transfected with indicated plasmids for 24 h, followed by SVCV challenge for 24 h.
875 The fluorescence intensity (arbitrary unit, a.u.) was recorded by the LAS X software,
876 and the data were expressed as mean ± SD, n = 5. (P) Schematic representation of full-
877 length Dtx4 and its mutants. (Q) IB of WCLs and proteins immunoprecipitated with
878 anti-Myc or HA Ab-conjugated agarose beads from EPC cells transfected with
879 indicated plasmids for 24 h. (R) TBK1 ubiquitination assays in EPC cells transfected
880 with indicated plasmids for 18 h, followed by MG132 treatments for 6 h.

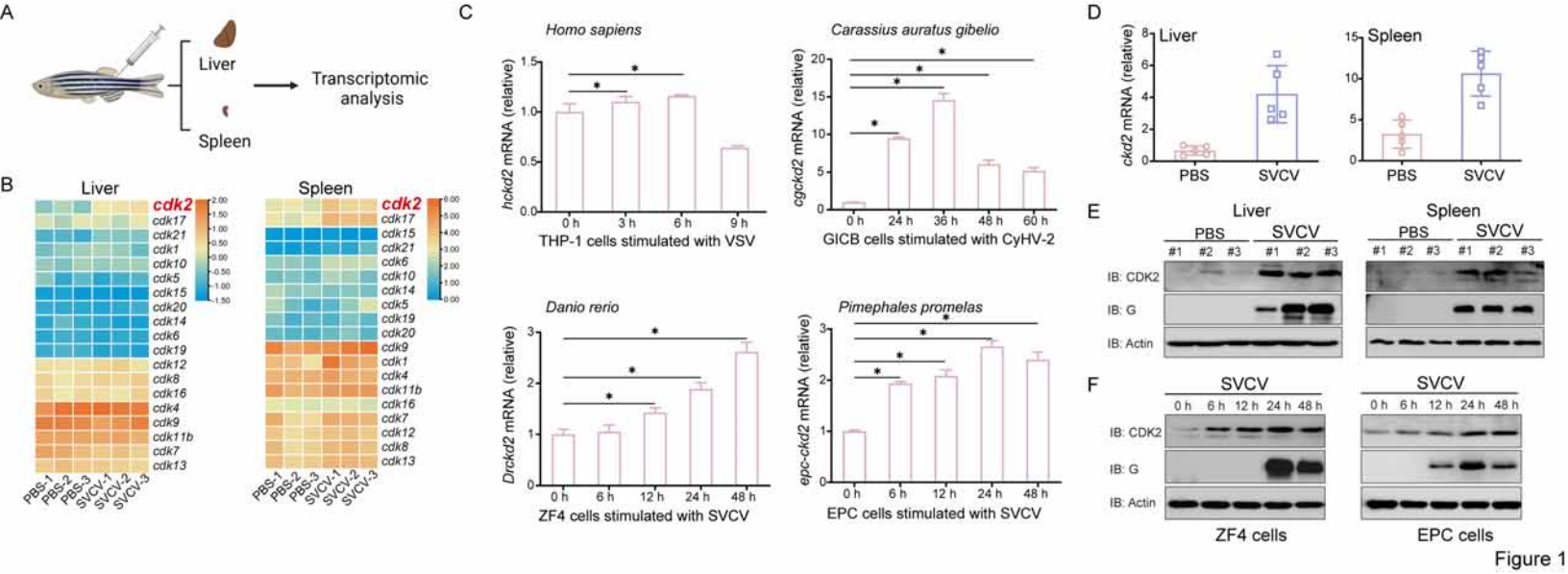
A
Liver
Spleen
Transcriptomic analysis
B
Liver
Spleen
cdk2
cdk17
cdk21
cdk1
cdk10
cdk5
cdk15
cdk20
cdk14
cdk6
cdk19
cdk12
cdk8
cdk16
cdk4
cdk9
cdk11b
cdk7
cdk13
PBS-1
PBS-2
PBS-3
SVCV-1
SVCV-2
SVCV-3
C
Homo sapiens
hckd2 mRNA (relative)
THP-1 cells stimulated with VSV
Carassius auratus gibelio
cgckd2 mRNA (relative)
GICB cells stimulated with CyHV-2
Danio rerio
Drckd2 mRNA (relative)
ZF4 cells stimulated with SVCV
Pimephales promelas
epc-ckd2 mRNA (relative)
EPC cells stimulated with SVCV
D
Liver
Spleen
ckd2 mRNA (relative)
PBS
SVCV
E
Liver
Spleen
PBS
SVCV
IB: CDK2
IB: G
IB: Actin
F
SVCV
0 h
6 h
12 h
24 h
48 h
ZF4 cells
EPC cells

Figure 1

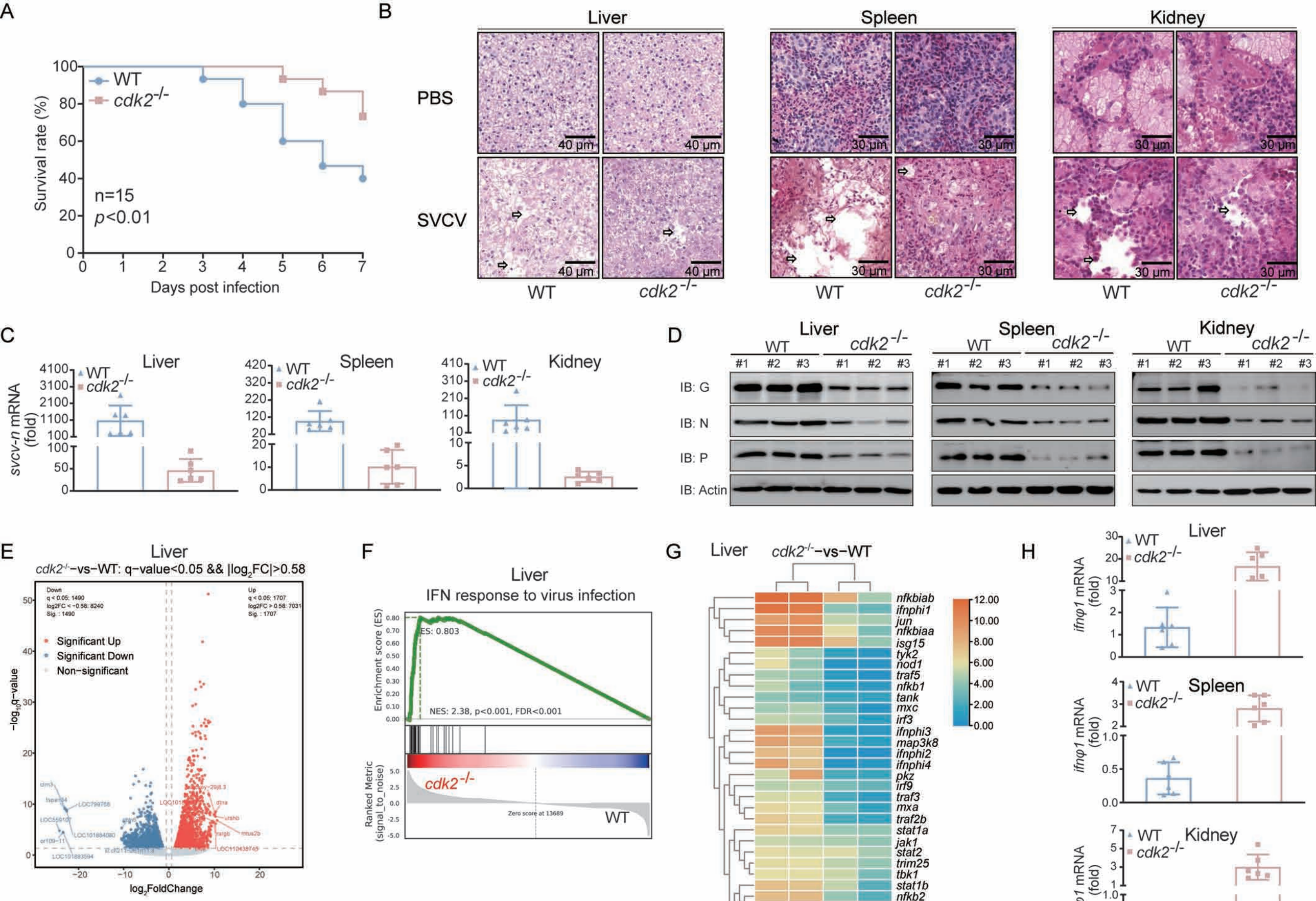
A
WT
cdk2-/-
Survival rate (%)
n=15
p<0.01
Days post infection
B
Liver
Spleen
Kidney
PBS
SVCV
WT
cdk2-/-
C
Liver
Spleen
Kidney
WT
cdk2-/-
svcv-n mRNA (fold)
D
Liver
Spleen
Kidney
WT
cdk2-/-
IB: G
IB: N
IB: P
IB: Actin
E
Liver
cdk2-/--vs-WT: q-value<0.05 && |log2FC|>0.58
Significant Up
Significant Down
Non-significant
log2FoldChange
F
Liver
IFN response to virus infection
ES: 0.803
NES: 2.38, p<0.001, FDR<0.001
Enrichment score (ES)
Ranked Metric (signal_to_noise)
cdk2-/-
WT
Zero score at 13689
G
Liver
cdk2-/--vs-WT
nfkbiab
ifnphi1
jun
nfkbiaa
isg15
tyk2
nod1
traf5
nfkb1
tank
mxc
irf3
ifnphi3
map3k8
ifnphi2
ifnphi4
pkz
irf9
traf3
mxa
traf2b
stat1a
jak1
stat2
trim25
tbk1
stat1b
nfkb2
mxe
mxb
irf7
H
Liver
Spleen
Kidney
WT
cdk2-/-
ifnφ1 mRNA (fold)

Figure 2

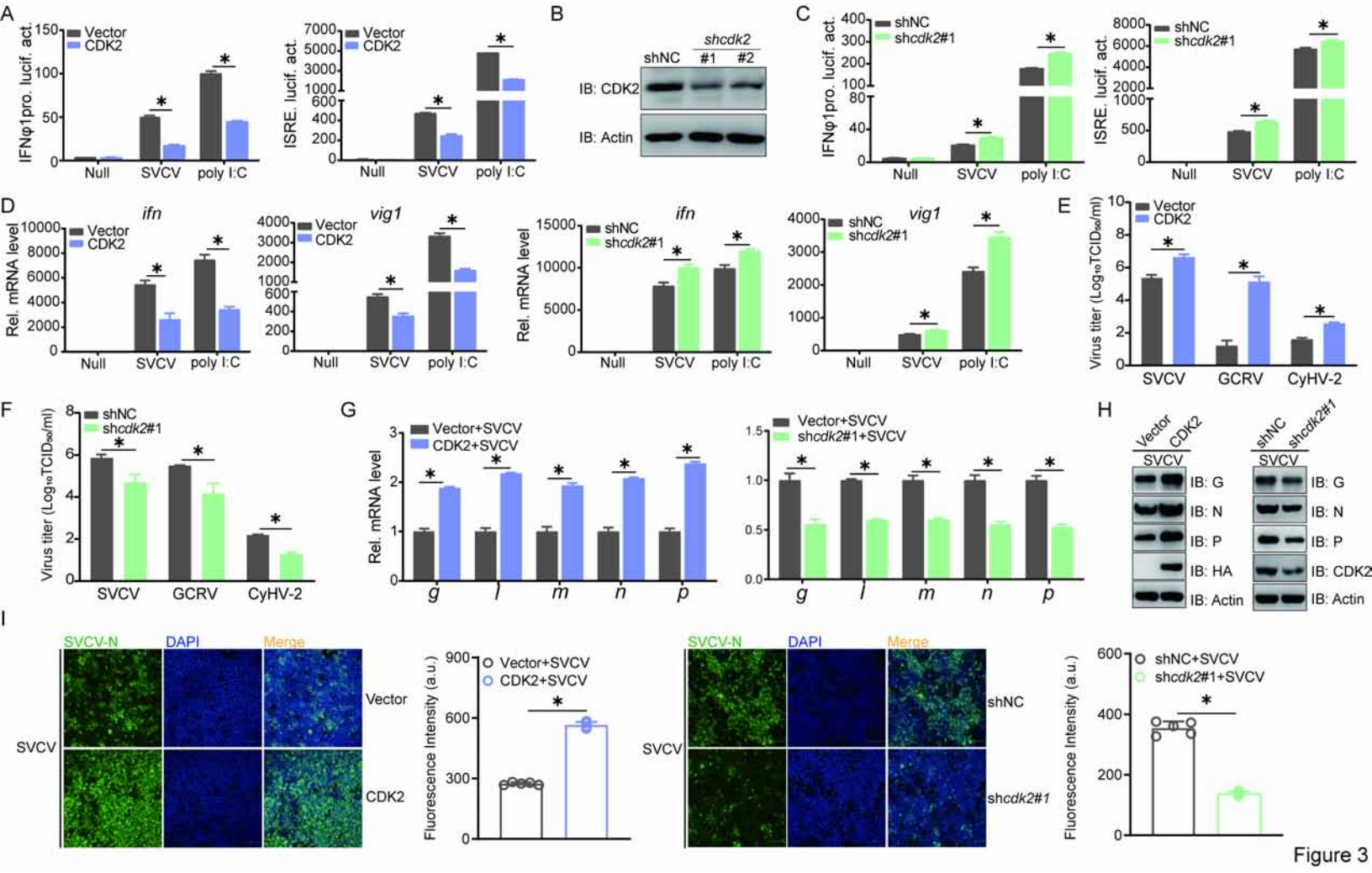
A
IFNφ1pro. lucif. act.
Vector
CDK2
Null
SVCV
poly I:C
ISRE. lucif. act.
B
shcdk2
shNC
#1
#2
IB: CDK2
IB: Actin
C
shNC
shcdk2#1
D
ifn
vig1
Rel. mRNA level
E
Virus titer (Log10TCID50/ml)
GCRV
CyHV-2
F
G
Vector+SVCV
CDK2+SVCV
shcdk2#1+SVCV
g
l
m
n
p
H
IB: G
IB: N
IB: P
IB: HA
IB: CDK2
I
SVCV-N
DAPI
Merge
Fluorescence Intensity (a.u.)
shNC+SVCV
shcdk2#1+SVCV

Figure 3

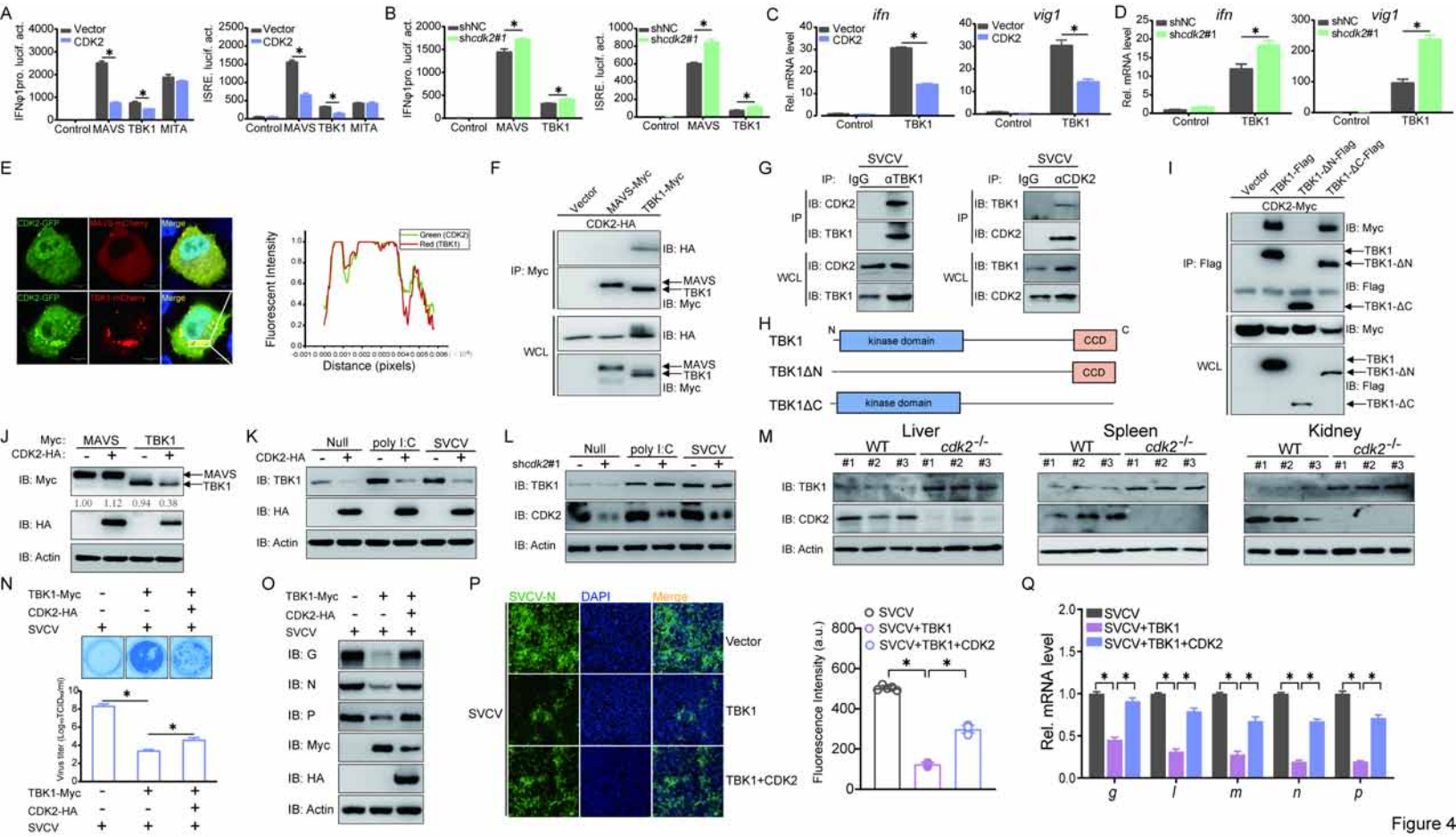
A
IFNφ1pro. lucif. act.
Vector
CDK2
Control MAVS TBK1 MITA
ISRE. lucif. act.
B
shNC
shcdk2#1
C
ifn
vig1
Rel. mRNA level
Control TBK1
D
E
CDK2-GFP
MAVS-mCherry
TBK1-mCherry
Merge
Green (CDK2)
Red (TBK1)
Fluorescent Intensity
Distance (pixels)
F
Vector
MAVS-Myc
TBK1-Myc
CDK2-HA
IP: Myc
IB: HA
IB: Myc
MAVS
TBK1
WCL
G
SVCV
IP: IgG αTBK1
IP: IgG αCDK2
IB: CDK2
IB: TBK1
H
TBK1
TBK1ΔN
TBK1ΔC
kinase domain
CCD
I
Vector
TBK1-Flag
TBK1-ΔN-Flag
TBK1-ΔC-Flag
CDK2-Myc
IP: Flag
IB: Flag
TBK1-ΔN
TBK1-ΔC
J
Myc: MAVS TBK1
CDK2-HA:
1.00 1.12 0.94 0.38
IB: Actin
K
Null
poly I:C
SVCV
L
shcdk2#1
M
Liver
Spleen
Kidney
WT
cdk2-/-
#1 #2 #3
N
TBK1-Myc
CDK2-HA
SVCV
Virus titer (Log10TCID50/ml)
O
IB: G
IB: N
IB: P
P
SVCV-N
DAPI
Merge
Vector
TBK1
TBK1+CDK2
Fluorescence Intensity (a.u.)
SVCV+TBK1
SVCV+TBK1+CDK2
Q
g
l
m
n
p

Figure 4

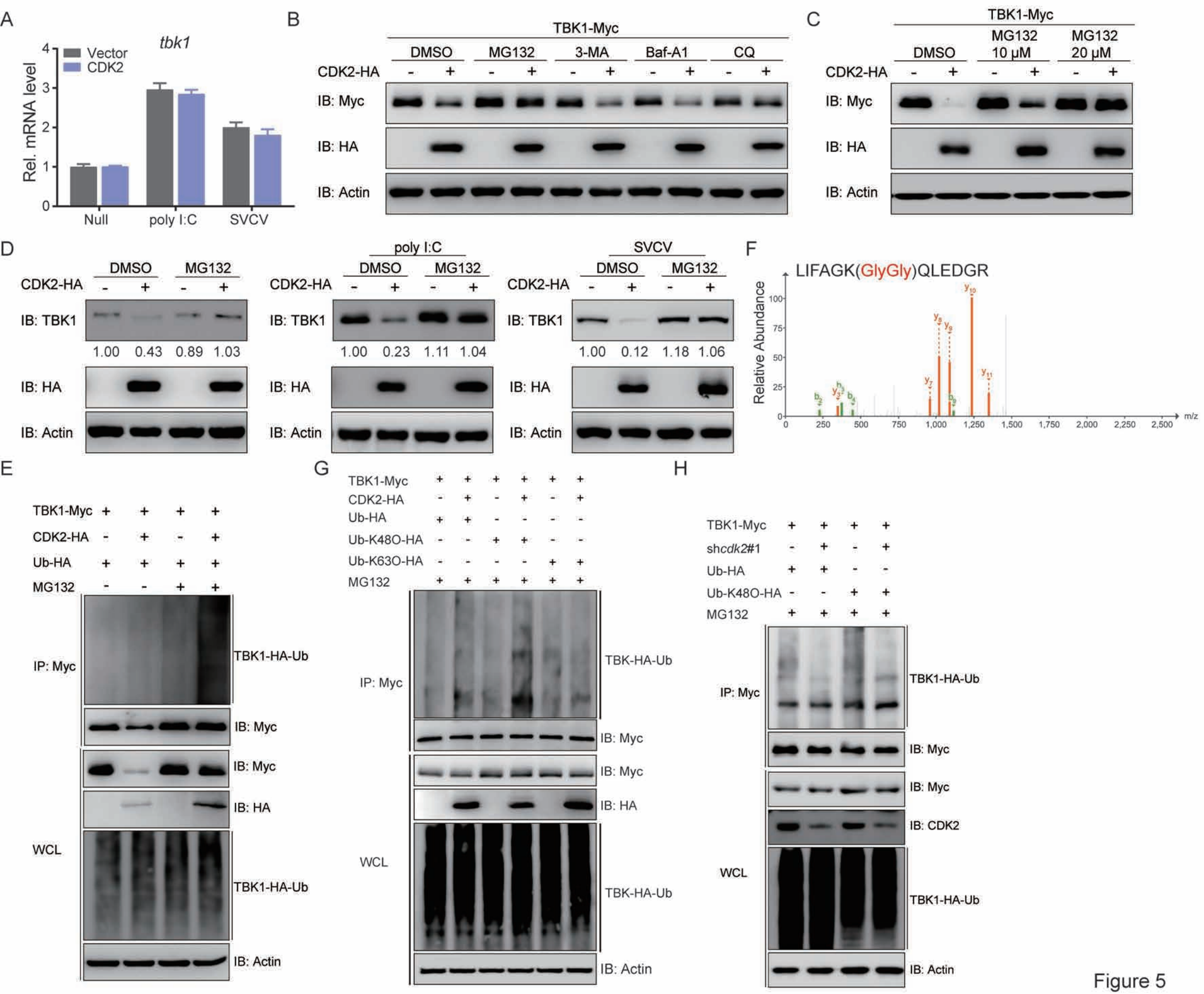
A
tbk1
Vector
CDK2
Rel. mRNA level
Null
poly I:C
SVCV
B
TBK1-Myc
DMSO
MG132
3-MA
Baf-A1
CQ
CDK2-HA
IB: Myc
IB: HA
IB: Actin
C
TBK1-Myc
DMSO
MG132 10 μM
MG132 20 μM
CDK2-HA
IB: Myc
IB: HA
IB: Actin
D
DMSO
MG132
CDK2-HA
IB: TBK1
1.00 0.43 0.89 1.03
IB: HA
IB: Actin
poly I:C
DMSO
MG132
CDK2-HA
IB: TBK1
1.00 0.23 1.11 1.04
IB: HA
IB: Actin
SVCV
DMSO
MG132
CDK2-HA
IB: TBK1
1.00 0.12 1.18 1.06
IB: HA
IB: Actin
F
LIFAGK(GlyGly)QLEDGR
Relative Abundance
m/z
E
TBK1-Myc
CDK2-HA
Ub-HA
MG132
IP: Myc
TBK1-HA-Ub
IB: Myc
IB: Myc
IB: HA
WCL
TBK1-HA-Ub
IB: Actin
G
TBK1-Myc
CDK2-HA
Ub-HA
Ub-K48O-HA
Ub-K63O-HA
MG132
IP: Myc
TBK-HA-Ub
IB: Myc
IB: Myc
IB: HA
WCL
TBK-HA-Ub
IB: Actin
H
TBK1-Myc
shcdk2#1
Ub-HA
Ub-K48O-HA
MG132
IP: Myc
TBK1-HA-Ub
IB: Myc
IB: Myc
IB: CDK2
WCL
TBK1-HA-Ub
IB: Actin

Figure 5

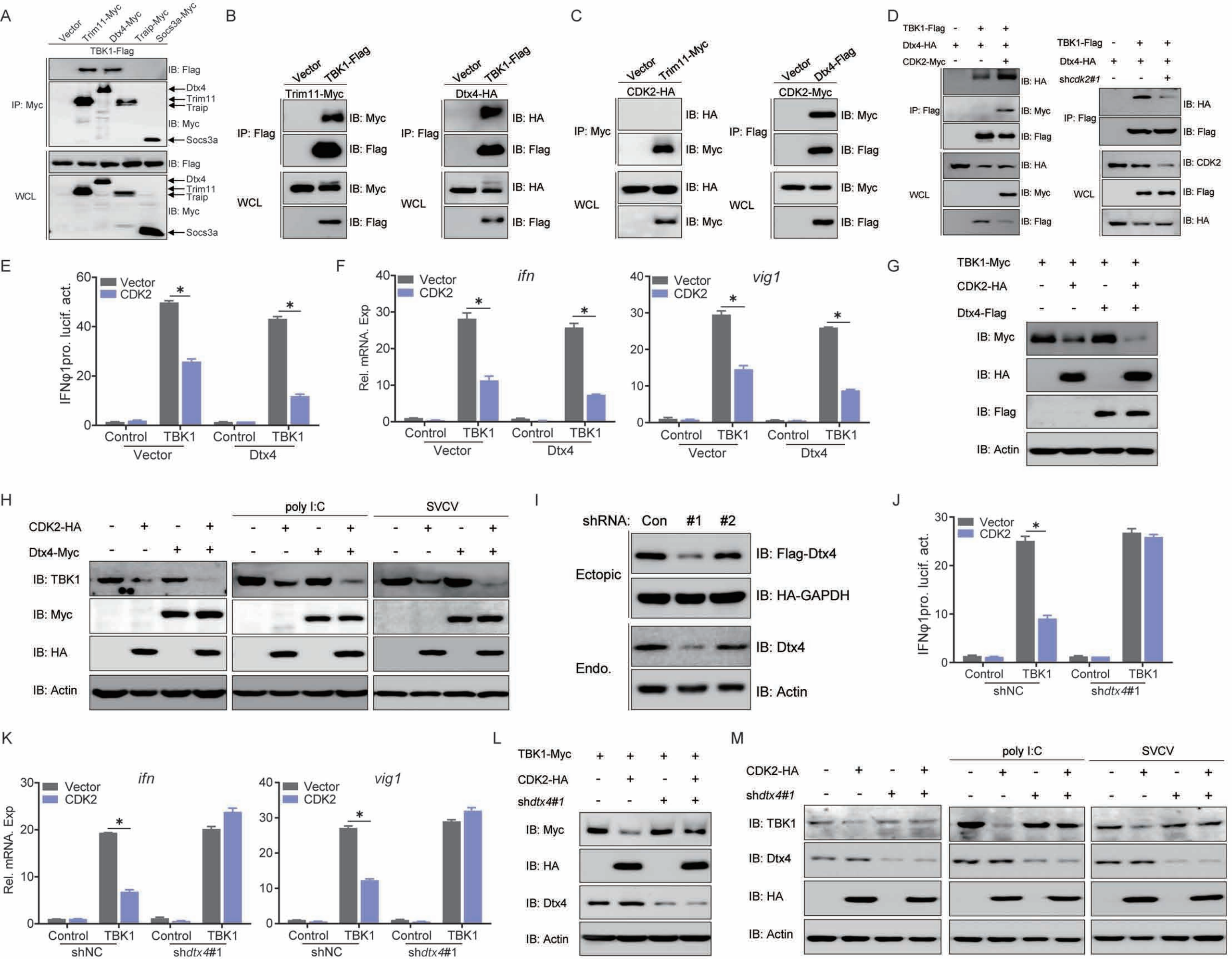
A
Vector
Trim11-Myc
Dtx4-Myc
Traip-Myc
Socs3a-Myc
TBK1-Flag
IP: Myc
WCL
IB: Flag
Dtx4
Trim11
Traip
IB: Myc
Socs3a
B
Vector
TBK1-Flag
Trim11-Myc
Dtx4-HA
IP: Flag
WCL
IB: Myc
IB: Flag
IB: HA
C
CDK2-HA
CDK2-Myc
Dtx4-Flag
D
TBK1-Flag
Dtx4-HA
CDK2-Myc
shcdk2#1
IB: HA
IB: CDK2
E
IFNφ1pro. lucif. act.
Vector
CDK2
Control
TBK1
F
Rel. mRNA. Exp
ifn
vig1
G
TBK1-Myc
CDK2-HA
Dtx4-Flag
IB: Actin
H
poly I:C
SVCV
Dtx4-Myc
IB: TBK1
I
shRNA:
Con
#1
#2
Ectopic
Endo.
IB: Flag-Dtx4
IB: HA-GAPDH
IB: Dtx4
J
shNC
shdtx4#1
K
L
M

Figure 6

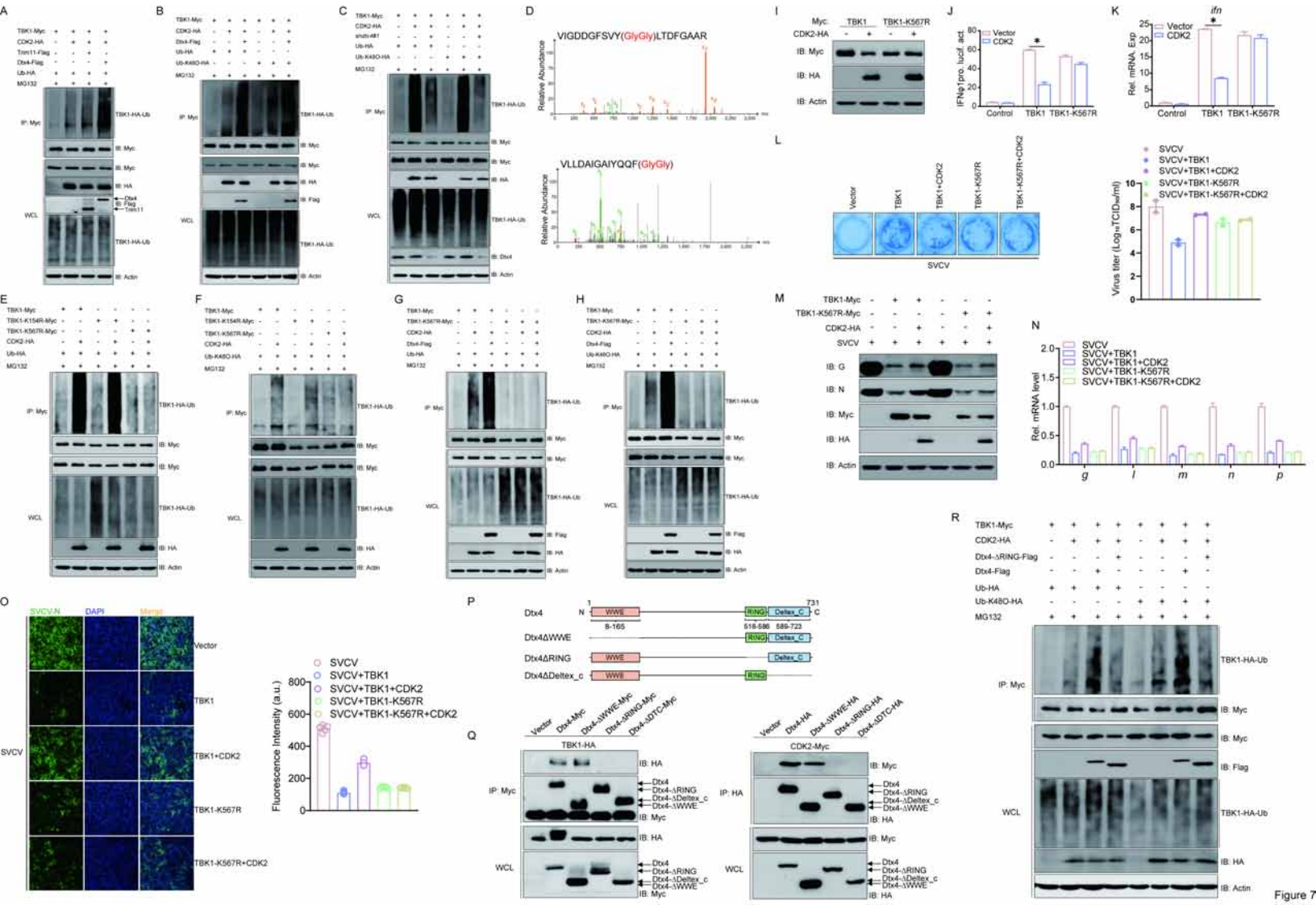
A
B
C
D
VIGDDGFSVY(GlyGly)LTDFGAAR
VLLDAIGAIYQQF(GlyGly)
Relative Abundance
I
Myc: TBK1 TBK1-K567R
CDK2-HA
IB: Myc
IB: HA
IB: Actin
J
Vector
CDK2
iFNβ1pro. lucif. act
Control TBK1 TBK1-K567R
K
ifn
Rel. mRNA Exp
L
Vector
TBK1
TBK1+CDK2
TBK1-K567R
TBK1-K567R+CDK2
SVCV
SVCV
SVCV+TBK1
SVCV+TBK1+CDK2
SVCV+TBK1-K567R
SVCV+TBK1-K567R+CDK2
Virus titer (Log10TCID50/ml)
E
F
G
H
M
TBK1-Myc
TBK1-K567R-Myc
CDK2-HA
SVCV
IB: G
IB: N
IB: Myc
IB: HA
IB: Actin
N
SVCV
SVCV+TBK1
SVCV+TBK1+CDK2
SVCV+TBK1-K567R
SVCV+TBK1-K567R+CDK2
Rel. mRNA level
g
l
m
n
p
O
SVCV-N
DAPI
Merge
Vector
TBK1
TBK1+CDK2
TBK1-K567R
TBK1-K567R+CDK2
SVCV
SVCV
SVCV+TBK1
SVCV+TBK1+CDK2
SVCV+TBK1-K567R
SVCV+TBK1-K567R+CDK2
Fluorescence Intensity (a.u.)
P
Dtx4
WWE
RING
Deltex_C
8-165
516-586
589-723
Dtx4ΔWWE
Dtx4ΔRING
Dtx4ΔDeltex_c
Q
Vector
Dtx4-Myc
Dtx4-ΔWWE-Myc
Dtx4-ΔRING-Myc
Dtx4-ΔDTC-Myc
TBK1-HA
IP: Myc
WCL
Dtx4-ΔRING
Dtx4-ΔDeltex_c
Dtx4-ΔWWE
Vector
Dtx4-HA
Dtx4-ΔWWE-HA
Dtx4-ΔRING-HA
Dtx4-ΔDTC-HA
CDK2-Myc
IP: HA
R
TBK1-Myc
CDK2-HA
Dtx4-ΔRING-Flag
Dtx4-Flag
Ub-HA
Ub-K48O-HA
MG132
IP: Myc
WCL
IB: Flag
IB: Actin

Figure 7